Moz and Retinoic Acid Coordinately Regulate H3K9 Acetylation, *Hox* Gene Expression, and Segment Identity

Anne K. Voss,[1,2,*] Caitlin Collin,[1] Mathew P. Dixon,[1] and Tim Thomas[1,2,*]
[1]The Walter and Eliza Hall Institute of Medical Research, Parkville, Victoria 3052, Australia
[2]Department of Medical Biology, The University of Melbourne, Parkville, Victoria 3050, Australia
*Correspondence: avoss@wehi.edu.au (A.K.V.), tthomas@wehi.edu.au (T.T.)

SUMMARY

We report that embryos deficient in the histone acetyltransferase Moz (Myst3/Kat6a) show histone H3 lysine 9 (H3K9) hypoacetylation, corresponding H3K9 hypermethylation, and reduced transcription at *Hox* gene loci. Consistent with an observed caudal shift in *Hox* gene expression, segment identity is shifted anteriorly, such that Moz-deficient mice show a profound homeotic transformation of the axial skeleton and the nervous system. Intriguingly, histone acetylation defects are relatively specific to H3K9 at *Hox* loci, as neither *Hox* H3K14 acetylation nor bulk H3K9 acetylation levels throughout the genome are strongly affected; H4K16 acetylation actually increases in the absence of Moz. H3K9 hypoacetylation, *Hox* gene repression, and the homeotic transformation caused by lack of Moz are all reversed by treatment with retinoic acid (RA). In conclusion, our data show that Moz regulates H3K9 acetylation at *Hox* gene loci and that RA can act independently of Moz to establish specific Hox gene expression boundaries.

INTRODUCTION

Vertebrates are structured into body segments, which are most obvious in the vertebral column, but also marked in the nervous system. In addition, during development structures such as the head and neck area and the kidneys are segmented. *Hox* genes confer body segment identity, first shown in *Drosophila melanogaster* by mutation or overexpression of one homeotic gene leading to complete misspecification of body segments such that, for example, a leg develops in the place of an antenna or visa versa (Schneuwly et al., 1987; Struhl, 1981). A single ancestral *Hox* gene cluster has undergone multiple rounds of duplications to form four Hox gene clusters in mammals (Pollard and Holland, 2000). Consequently, the roles of *Hox* genes in body segment identity specification in mammals show some degree of redundancy. Mutations of *Hox* genes are partially compensated by the paralogous *Hox* genes in the other clusters (Condie and Capecchi, 1994; Fromental-Ramain et al., 1996; Horan et al., 1995). Therefore, dramatic homeotic transformations as seen in *Drosophila* are rare in mammals. While *Hox* gene mutant phenotypes clearly demonstrate the roles of *Hox* genes in body segment identity specification, they do not resolve how the *Hox* gene expression patterns are established and maintained specifically with respect to segment boundaries.

Homeotic transformations have led to the identification of regulators of *Hox* gene expression, proteins of the trithorax (TrxG) and polycomb group (PcG) (reviewed by Deschamps and van Nes, 2005; Ringrose and Paro, 2004). It is thought that TrxG and PcG proteins affect *Hox* gene expression by modifying chromatin structure, introducing covalent modifications to the amino-terminal tails of histones in the *Hox* clusters. PcG proteins add the transcriptional repression mark trimethylation of lysine 27 of histone 3 (H3K27me3) (Ringrose et al., 2004). In contrast, TrxG proteins add the transcriptional activation mark trimethylation of lysine 4 on histone 3 (H3K4me3) (Nakamura et al., 2002). In this manner PcG and TrxG may repress and activate/maintain *Hox* gene expression, respectively (Lachner and Jenuwein, 2002; Ringrose and Paro, 2004). However, it is unclear precisely how lysine modification by PcG and TrxG proteins leads to repression and activation of transcription, respectively (Ringrose and Paro, 2007). Transcriptionally active loci exhibit acetylation of lysines in the amino-terminal tails of histones (e.g., H3K9ac; H3K14ac; H4K5ac; H4K16ac) in addition to H3K4me3 (Jenuwein and Allis, 2001). Therefore, proteins with histone acetyltransferase activity must be involved in the global regulation of *Hox* gene expression. We show here that the MYST protein, monocytic leukemia zinc finger protein (Moz), regulates histone acetylation at *Hox* gene loci and their expression.

The human *MOZ* gene was first identified in recurrent t(8;16)(p11;p13) translocations causing a particularly aggressive form of acute myeloid leukemia (FAB M4/5) (Borrow et al., 1996). Subsequently, other *MOZ* mutations were discovered in leukemia and myelodysplastic syndrome (Carapeti et al., 1998; Chaffanet et al., 2000; Esteyries et al., 2008; Liang et al., 1998). Mouse fetuses lacking the *Moz* gene do not have definitive hematopoietic stem cells as assessed by competitive reconstitution assays, and, as a consequence, $Moz^{\Delta/\Delta}$ fetuses are deficient in multipotent progenitors and all lineage-specific hematopoietic progenitors (Katsumoto et al., 2006; Thomas et al., 2006). Human leukemia cases involving *MOZ* translocations and the *Moz* mutant phenotype in mice show that *Moz* has an important role in the development of hematopoietic stem cells and the regulation of hematopoiesis. However, the molecular mechanism of Moz function is unclear.

The Moz protein has a central MYST histone acetyltransferase domain, which it shares with the other four mammalian MYST

family members (Thomas and Voss, 2007; Voss and Thomas, 2009). Amino-terminal to this are two plant homeodomain zinc fingers (PHD) and an amino-terminal NEMM domain. Moz has carboxy-terminal serine- and methionine-rich domains with transactivation properties in vitro (Champagne et al., 2001; Kitabayashi et al., 2001). MOZ can interact with acute myeloid leukemia protein 1 (AML1/RUNX1) and with PU.1 and enhances AML1 as well as PU.1-induced transcriptional activation in vitro (Katsumoto et al., 2006; Kitabayashi et al., 2001). However, *Moz* is a widely expressed gene in adult tissues as well as during development and is therefore likely to regulate a wide range of biological processes both within the hematopoietic system and in other cell types.

MOZ can acetylate all core histones in vitro (Champagne et al., 2001; Holbert et al., 2007; Laue et al., 2008). However, when isolated from HeLa cells as a component of the ING5 tumor suppressor complex, MOZ shows specificity for H3K14 acetylation in vitro (Doyon et al., 2006). Another study suggested that MOZ specifically acetylates H4K16 (Fraga et al., 2005), indicating considerable uncertainty as to which lysine residues Moz may acetylate. Moreover, the preference of Moz for specific lysine residues in vivo has not been examined and there is no functional evidence linking histone acetyltransferase function of Moz at specific lysine residues to transcriptional regulation in vivo.

Mutation of the *Moz* homolog in zebrafish causes cranial neural crest development defects (Crump et al., 2006; Miller et al., 2004). Interestingly, effects of zebrafish *moz* mutation are restricted to the head region. In contrast, in mice, as we report here, mutation of the *Moz* gene causes an anterior homeotic transformation of 19 body segments of the neck and trunk region, a homeotic transformation unusual in extent and completeness in mammals. The *Moz* mutant anterior homeotic transformation was completely rescued by RA treatment. We show that Moz is required for normal levels of expression of all *Hox* genes examined and for the establishment of the correct anterior expression boundary of *Hox* genes 5′ of the second paralogous group. Furthermore and in contrast to previous in vitro data, we found that Moz is essential for H3K9 acetylation in vivo.

RESULTS

Mutation of *Moz* Causes an Anterior Homeotic Transformation

Moz$^{\Delta/\Delta}$ mutant mouse pups (Thomas et al., 2006) exhibit a hunched posture and an extended neck region at birth (Figures 1A and 1B). Examination of skeletal preparations revealed the presence of an additional 8th cervical vertebra in all *Moz*$^{\Delta/\Delta}$ mutant pups, whereas all wild-type and *Moz*$^{\Delta/+}$ heterozygous pups had the normal complement of seven cervical vertebrae (Figures 1C–1F; n = 10 *Moz*$^{\Delta/\Delta}$ mutant and 11 wild-type pups). The additional cervical vertebra had the morphology of a supernumerary first vertebra, the atlas (Figures 1G and 1H). In the *Moz*$^{\Delta/\Delta}$ mutants the first and the secondary atlas shared one common enlarged anterior arch of the atlas (Figures 1C and 1D). The shift in axial skeleton segment identity in the *Moz*$^{\Delta/\Delta}$ mutants was perpetuated throughout the cervical and thoracic vertebrate column, such that the 8th vertebra, which is ordinarily the first rib-bearing thoracic vertebra, acquired the morphology of the seventh cervical vertebra. Occasionally it had small bones attached to its ventral side. Smaller rudimentary ribs have been observed at the 7th cervical vertebra in 40% of

wild-type pups (Kessel and Gruss, 1991). The 9th vertebra, which forms the second thoracic vertebra in wild-types and *Moz*$^{\Delta/+}$ heterozygotes, was the first vertebra in the *Moz*$^{\Delta/\Delta}$ mutants carrying a normal rib with contact to the sternum (Figures 1G and 1H). *Moz*$^{\Delta/\Delta}$ mutants exhibited only 12 rib-bearing thoracic vertebra as compared to the normal complement of 13 in wild-types and *Moz*$^{\Delta/+}$ heterozygotes, such that the first lumbar vertebra is the first vertebra correctly specified in the *Moz*$^{\Delta/\Delta}$ mutants (data not shown).

Paralleling the additional cervical axial skeleton segment, we observed an additional cervical segment in the nervous system. E10.5 embryos stained for neurofilament marked 3 occipital, 7 cervical, 13 thoracic, and also lumbar and caudal intersegmental nerves clearly in the wild-type (Figure 1I). The first intersegmental nerve contributing to the innervation of the forelimb is the 7th intersegmental nerve, which corresponds to the 4th cervical nerve. In contrast, the 8th intersegmental nerve was the first that contributed to the innervation of the forelimb in *Moz*$^{\Delta/\Delta}$ mutant embryos (Figure 1J, n = 6 wild-type and 6 *Moz*$^{\Delta/\Delta}$ mutant embryos). In the wild-types the first 4 intersegmental nerves contributed to the hypoglossal nerve (Figure 1K). In contrast in the *Moz*$^{\Delta/\Delta}$ mutants, the first 5 intersegmental nerves contributed to the hypoglossal nerve (Figure 1L). Interestingly, the effects of Moz were surprisingly specific to the process of determining body segment identity given the widespread expression of the *Moz* gene (see Figure S1 online).

Our data show that Moz deficiency results in a complete anterior homeotic transformation affecting C2 to T13 unusual in its completeness for mammals or vertebrates in general.

Moz Regulated *Hox* Genes Globally

The anterior homeotic transformation suggested that Moz either regulated *Hox* gene expression or acted as a transcriptional coregulator for Hox proteins. The extent and completeness of the homeotic transformation suggested that loss of Moz affected the function of a large number of *Hox* genes or proteins. We examined *Hox* genes of the A and of the B cluster, namely, *Hoxa1*, *a2*, *a3*, *a4*, *a5*, and *a6*, and *Hoxb2*, *b3*, *b4*, *b5*, *b6*, and *b8*. We observed that all *Hox* genes examined were expressed at lower levels in the *Moz*$^{\Delta/\Delta}$ mutant embryos as compared to wild-type controls by whole-mount in situ hybridization (Figures 2 and 3; n = 72 *Moz*$^{\Delta/\Delta}$ mutant embryos and 72 wild-type embryos). The difference was particularly prominent in *Hoxa1*, *Hoxa3*, *Hoxb3*, and *Hoxb4* (Figure 2A versus Figure 2B, Figure 2E versus Figure 2F and Figure 3C versus Figure 3D, Figure 3E versus Figure 3F).

Importantly, we observed a shift in the anterior expression boundary of all *Hox* genes 5′ of the second paralogous group. While the expression domains of *Hoxa1*, *Hoxa2*, and *Hoxb2* were not altered, the expression domains of *Hoxa3* to *Hoxa6* (Figure 2), *Hoxb3* to *Hoxb6*, and *Hoxb8* (Figure 3) were shifted by at least one body segment both in the paraxial mesoderm and in the nervous system (summarized in Figure 4A and Figure S2; n = 6 *Moz*$^{\Delta/\Delta}$ mutant embryos and 6 wild-type embryos per gene). As the expression levels of *Hoxb4* were too low in most *Moz*$^{\Delta/\Delta}$ mutant embryos to determine the anterior expression boundary, we examined Hoxb4 protein and observed the shift of the anterior expression boundary at the protein level (Figures 3M and 3N; n = 6 *Moz*$^{\Delta/\Delta}$ mutant embryos and 6 wild-type embryos).

Generally, the levels of *Hox* gene expression were more uniform among the wild-type embryos than in the *Moz*$^{\Delta/\Delta}$ mutant
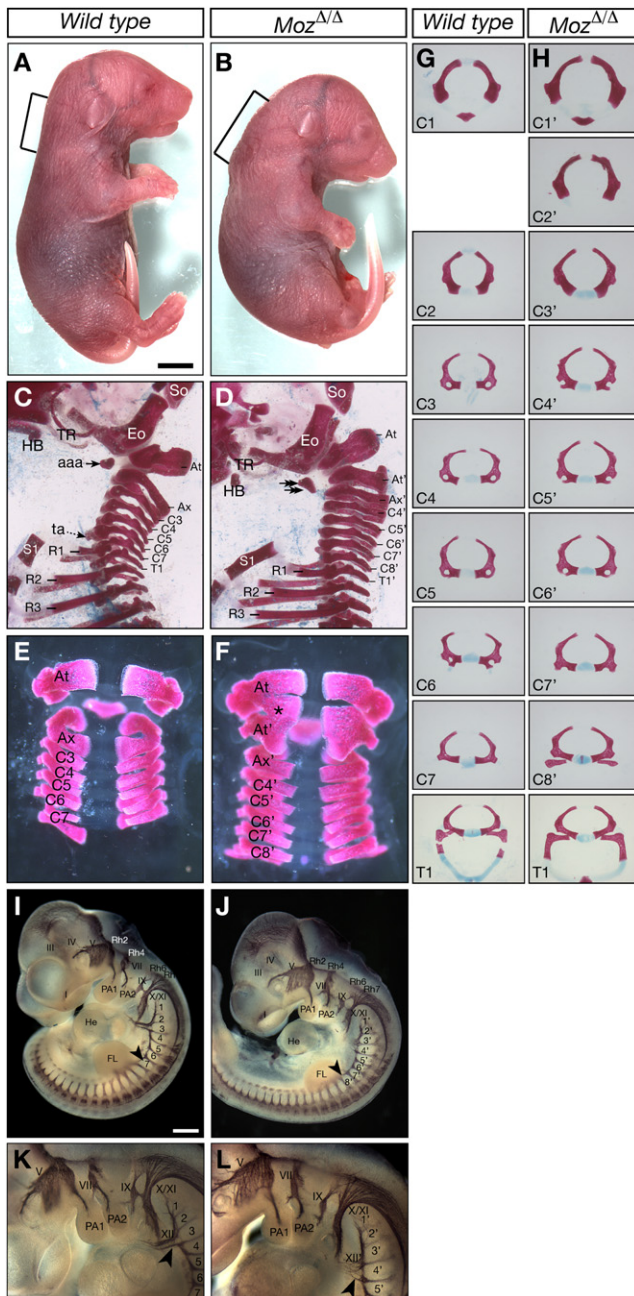
Figure 1. *Moz*^{Δ/Δ} Pups Have an Anterior Homeotic Transformation of the Axial Skeleton and the Nervous System

E18.5 (A–H) and E10.5 (I–L) wild-type (A, C, E, G, I, and K) and *Moz*^{Δ/Δ} (B, D, F, H, J, and L). Shown are the external appearance (A and B) and skeletal preparations of the cervical vertebrae column: lateral view (C and D), dorsal view (E and F), and axial, rostral view of individual cervical vertebra (G and H). Neurofilament immunostaining displays the segmental nerves along the body axis (J–L). Note the hunched posture and elongated neck region (bracket in [B] versus [A]). *Moz*^{Δ/Δ} mutant pups have eight instead of seven cervical vertebrae (C–H). The additional cervical vertebra is most similar to the morphology of the atlas (C, D, G, and H). The first and the supernumerary atlas share one enlarged anterior arch of the atlas (solid arrows in [D] versus [C]). The identities of all other cervical vertebrae are shifted to anterior by one segment (G and H). The tuberculum anterior is absent in the *Moz*^{Δ/Δ} (stippled arrow in [C] and [D]). In some *Moz*^{Δ/Δ} pups additional arches or partial arches of supernumerary

atlases can be observed (asterisk in [F] versus [E]). The first nerve contributing to the innervation of the forelimb is the 7th intersegmental nerve in the wild-type and the 8th in the *Moz*^{Δ/Δ} (arrowheads in [J] versus [I]). The first five intersegmental nerves contribute to the hypoglossal nerve (XII) in *Moz*^{Δ/Δ} as compared to the first four in wild-type (arrowheads in [L] versus [K]). I–XII, 1st to 12th cranial nerve; 1–8, 1st to 8th intersegmental nerve; aaa, anterior arch of the atlas; At, Atlas; At', supernumerary atlas; Ax, axis; C3–C7, 3rd to 7th cervical vertebrae; Ax', C4'–C8', axis and C4 to C8 in the *Moz*^{Δ/Δ} (prime indicates that these differ from the wild-type vertebrae); Eo, exooccipital bone; FB, forebrain; FL, forelimb; HB, hyoid bone; He, heart; PA1, PA2, 1st, 2nd pharyngeal arch; R1–R3, 1st to 3rd rib; Rh2–Rh7, rhombomeres 2 to 7; T1, T1', 1st thoracic vertebra; ta, tuberculum anterior; TR, tympanic ring; S1, 1st bone segment of the sternum; So, supraoccipital bone. Scale bar equals 2.5 mm in (A) and (B), 1.9 mm in (C) and (D), 0.6 mm in (E) and (F), 1.3 mm (G) and (H), 500 μm in (I) and (J), and 300 μm in (K) and (L).
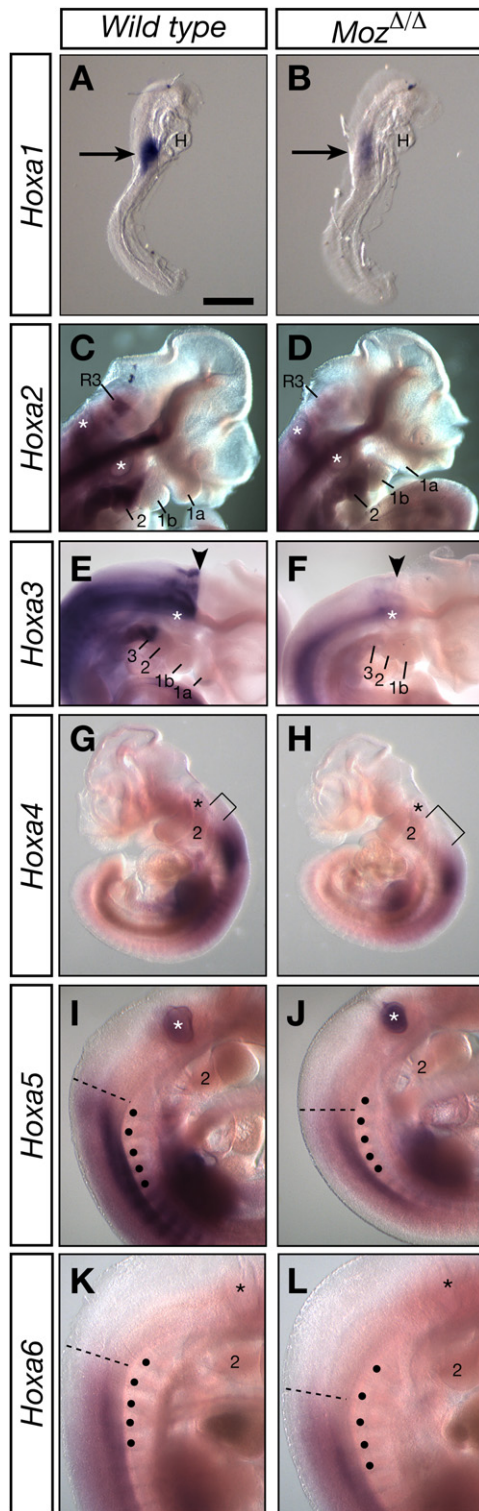
---

embryos and were almost undetectable in some *Moz*^{Δ/Δ} mutants (e.g., Figures 3D and 3F). Quantitation of *Hoxa3*, *Hoxa4*, *Hoxb3*, and *Hoxb4* mRNA by northern blot and densitometry at E9.5, E10.5 (Figure 4B), and E11.5 (Figures 4C and 4D) revealed an overall reduction in expression of these *Hox* genes in *Moz*^{Δ/Δ} mutant embryos by approximately one half. Analysis of three to five E11.5 embryos per genotype showed that the reduction in *Hox* gene expression was statistically significant (p < 0.0001) and that *Hoxb3* and *Hoxb4* mRNA was present in heterozygous *Moz*^{Δ/+} embryos at levels intermediate between wild-type and *Moz*^{Δ/Δ} homozygous embryos (Figure 4D).

Examining if *Hox* gene expression was initiated normally in *Moz*^{−/−} mutant embryos using the example of *Hoxa3*, we found that *Hoxa3* expression was very low or undetectable in E7.5 *Moz*^{−/−} mutant embryos as compared to controls and did not reached normal levels of expression at later stages (Figures 4E–4J; n = 8 *Moz*^{−/−} mutants and 9 littermate controls).

Our results show a global effect of *Moz* deletion on *Hox* gene expression and specification of the anterior expression boundary of *Hox* genes.

H3K9 Is Hypoacetylated and Hypermethylated at *Hox* Gene Loci in the Absence of Moz

To assess the effects of Moz deficiency on histone acetylation in E10.5 embryos, we determined the association of regions of the *Hoxa* and the *Hoxb* gene clusters (Figure 5A) with acetylated histones by chromatin immunoprecipitation using antibodies against acetylated H3K9 and H3K14 followed by quantitative genomic PCR. As H3K9 can be either acetylated (associated with transcription) or methylated (associated with silencing), we also examined H3K9 trimethylation levels. Data are presented normalized for the housekeeping gene *beta-2-microglobulin* for the activation marks (H3K9ac and H3K14ac) and for the transcriptionally repressed genes *albumin* and *hemoglobin beta 1* for the silencing mark (H3K9me3) within samples (n = 6 mutants and 6 controls for H3K9ac and H3K14ac; 3 mutants and 3 controls for H3K9me3). Based on the work of Doyon et al. (2006), we expected that H3K14 acetylation might be reduced in the absence of Moz and that H3K9 acetylation might be unchanged. Contrary to this expectation, we found that overall association of *Hox* gene sequences with acetylated H3K9 was significantly reduced in the *Moz* mutant embryos (Figures 5B–5E; p < 0.0001). Specifically, we found that genomic sequences significantly underrepresented in the *Moz* mutant anti-H3K9ac

Figure 2. *Moz*$^{\Delta/\Delta}$ Show Reduced Expression of all *Hoxa* Cluster Genes and a Posterior Shift in *Hoxa* Gene Expression from the 3rd Gene Onward

Wild-type (A, C, E, G, I, and K) and *Moz*$^{\Delta/\Delta}$ (B, D, F, H, J, and L) at E8.5 (A and B) and E10.5 (C–L). In situ hybridization detected *Hoxa1* to *Hoxa6* mRNA as indicated. E10.5 *sense* control experiments did not produce a signal (data not shown). Note the weaker signal in the *Moz*$^{\Delta/\Delta}$, in particular *Hoxa1* (arrows [B] versus [A]).

precipitate comprised the start of transcription of *Hoxa4*, *Hoxb3*, and *Hoxb4* (Figure 5B), the sequences 0.7 to 1.5 kb upstream of the start of transcription of *Hoxa4* and *Hoxb4* (Figure 5C), the coding regions (Figure 5D), and two putative retinoic acid response elements (RARE; Figure 5A and Table S1) each near the *Hoxa3* and *Hoxb3* loci (Figure 5E). Exact p values for the specific genomic sites examined by ChIP (Figure 5) are given in Table S2. While H3K9 hypoacetylation at the *Hox* loci was prominent, global levels of H3K9 acetylation were not significantly different in *Moz*$^{-/-}$ mutant, *Moz*$^{-/+}$ heterozygous, and wild-type embryos as assessed by immunoblotting and densitometry (Figures 5F and 5G; n = 3 embryos per genotype, 1 individual embryo per lane, p = 0.7109).

Mirroring the reduction in H3K9 acetylation, we observed an increase in H3K9me3 in *Moz*$^{-/-}$ mutant E10.5 embryos as compared to wild-type controls (Figures 5H and 5I; p = 0.0004). In contrast to H3K9ac, levels H3K14 acetylation were not significantly different between *Moz*$^{-/-}$ mutants and controls (Figures 5J–5M; p = 0.7155).

The differential effect on H3K9 and H3K14 acetylation suggests that the observed loss of histone acetylation at *Hox* loci is not merely a downstream consequence of transcriptional repression, but a direct and specific effect, as Moz deficiency does not affect all histone marks corresponding to gene activation at *Hox* loci. Overall our data indicate that in E10.5 mouse embryos Moz is required for normal levels of H3K9 acetylation across the *Hoxa* and the *Hoxb* gene clusters and has no or very limited effects on H3K14 acetylation.

Retinoic Acid Treatment Rescues the *Moz* Mutant Body Segment Identity Defect

Retinoic acid (RA) is a potent activator of *Hox* gene expression. Oversupply of RA or vitamin A leads to birth defects in humans (Geelen, 1979). In experimental settings, RA treatment of pregnant mice activates stronger as well as ectopic *Hox* gene expression in the developing embryos and causes homeotic transformations (Kessel and Gruss, 1991).

As the anterior homeotic transformation in *Moz* mutants was the opposite phenomenon to the posterior homeotic transformation after treatment with RA at E7, a connection between Moz and RA in body segment identity specification was possible. Therefore, we examined the effects of RA treatment on the Moz-deficient body segment identity defect (Figure 6; n = 11 *Moz*$^{\Delta/\Delta}$ homozygous, 12 *Moz*$^{\Delta/+}$ heterozygous, and 15 wild-type pups). Treatment of pregnant females with 10 μg/g bodyweight RA at E7.25 caused a posterior homeotic transformation in 8 of 9 wild-type pups, which developed only 6 cervical vertebra (Figures 6C and 6E), as reported previously (Kessel and Gruss, 1991). Notably, RA treatment at 10 μg/g completely rescued the Moz-deficient body segment identity defect in 6 of 6 *Moz*$^{\Delta/\Delta}$ mutant pups (Figures 6D and 6E). In one *Moz*$^{\Delta/\Delta}$ mutant pup,

and *Hoxa3* ([F] versus [E]). The anterior expression boundary in the neural tube is indicated (arrows in [E] and [F], dotted lines in [I]–[L], distance from the otic vesicle in [G] and [H]). Very weak expression of *Hoxa2* in the 3rd rhombomere in *Moz*$^{\Delta/\Delta}$ is indicated (R3 in D versus C). 1a, 1b, maxillary and mandibular part of the 1st pharyngeal arch; 2, 3, 2nd and 3rd pharyngeal arch; ●, prevertebrae; *, otic vesicle. Scale bars equal 550 μm in (A) and (B), 455 μm in (C), (D), (K) and (L), 755 μm in (E) and (F), 1.2 mm in (G) and (H), and 485 μm in (I) and (J).
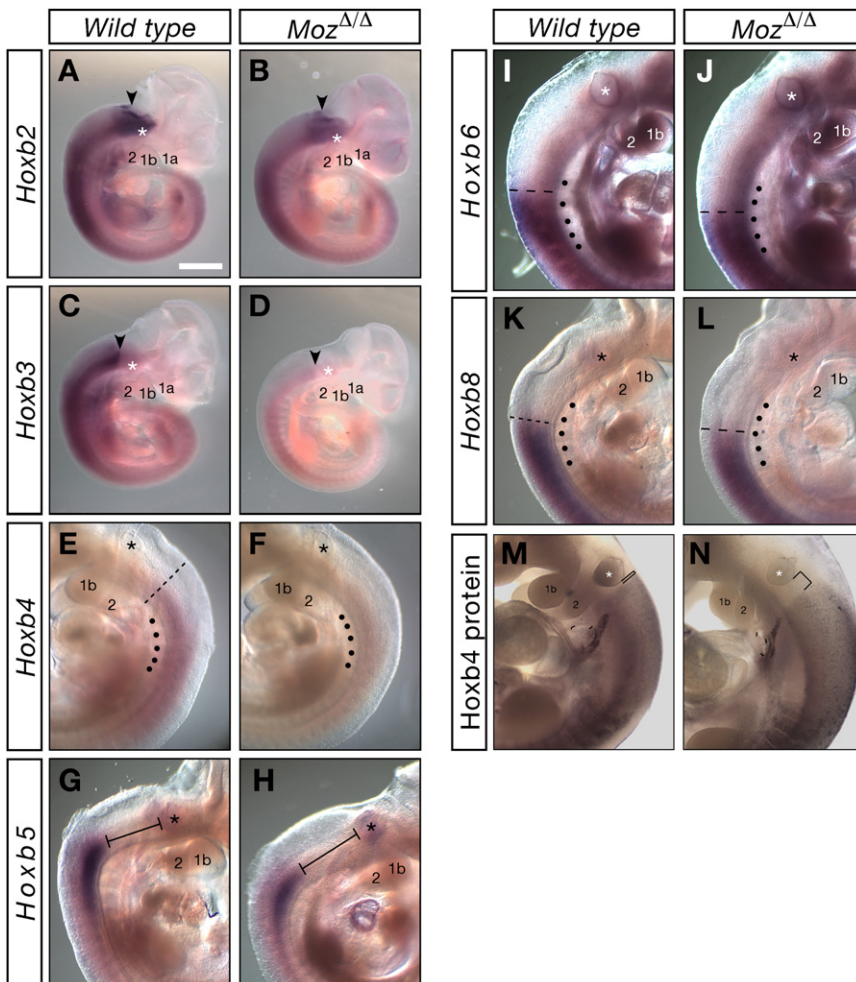
Figure 3. *Moz^{Δ/Δ}* Show Reduced Expression of All *Hoxb* Cluster Genes and a Posterior Shift in *Hoxb* Gene Expression from the 3rd Gene Onward

E10.5 wild-type (A, C, E, G, I, K, and M) and *Moz^{Δ/Δ}* (B, D, F, H, J, L, and N). In situ hybridization (A–L) detecting *Hoxb2* to *Hoxb6* and *Hoxb8* mRNA as indicated. Note the weaker signal in the *Moz^{Δ/Δ}*, in particular *Hoxb3* (C and D) and *Hoxb4* (F) versus [E]). Hoxb4 protein distribution is shown (M and N). The anterior expression boundary in the neural tube is indicated (arrows in [A]–[D], dotted lines in [E], [F], and [I]–[L], and distance from the otic vesicle in [G], [H], [M], and [N]). Labeling is as in Figure 2. Scale bar equals 1.1 mm in [A]–[D], 390 μm in [E], [F], [M], and [N], 725 μm in [G] and [H], 340 μm in [I] and [J], and 390 μm in [K] and [L].

protein occurred normally in the reported RA signaling domain (data not shown; n = 3 *Moz^{Δ/Δ}* mutant embryos and 3 wild-type embryos). Therefore, Moz is not required for RAR expression or nuclear translocation. We conclude that essential elements of RA signaling are normal in *Moz^{Δ/Δ}* mutant embryos. Furthermore, RA signaling rescues the *Moz* mutant body segment identity defect in the absence of Moz, suggesting that RA acts in parallel to Moz to define body segment identity.

Retinoic Acid Treatment Restores H3K9 Acetylation at *Hox* Gene Loci in Moz Mutants

As RA rescued the *Moz* mutant segment identity defect (Figure 6) and *Hox* gene expression (Figure S3), we predicted that RA would rescue the deficiency in histone acetylation in *Moz* mutant embryos. Indeed, H3K9 acetylation returned to normal levels in E10.5 *Moz^{−/−}* mutant embryos that were treated with RA at E9.5 (Figure 7; n = 5 RA-treated *Moz* mutants, 4 RA-treated wild-type controls, 5 untreated *Moz* mutants and 4 untreated wild-type control embryos). As in our previous series of experiments, H3K9ac was reduced in untreated *Moz^{−/−}* mutant embryos as compared to controls at sites upstream of the start of transcription of *Hoxa4* and *Hoxb4* (Figure 7A) and at the RARE (Figure 7B). RA treatment resulted in a significant increase in H3K9ac in *Moz^{−/−}* mutants embryos (p < 0.0001) such that the levels were no longer significantly different from controls upstream of the start of transcription (Figure 7C versus Figure 7A) and at RARE (Figure 7D versus Figure 7B). Exact p values for individual genomic sites are displayed in Table S3.

In contrast to H3K9 acetylation, H3K14 acetylation was neither affected by the absence of Moz (Figure 7F), nor by treatment with RA (Figure 7G), indicating that not all acetylation marks are regulated by Moz and RA.

Surprisingly, we observed that H4K16 acetylation was increased in *Moz^{−/−}* mutant embryos compared with controls with or without

RA overcompensated for the Moz defect (Figure 6E). A reduced RA dose of 5 μg/g rescued the *Moz* mutant phenotype in 4 of 5 *Moz^{Δ/Δ}* mutant embryos (Figure 6E). Interestingly, *Moz^{Δ/+}* heterozygous embryos showed a response intermediate between wild-type and *Moz^{Δ/Δ}* homozygous embryos. One half of the *Moz^{Δ/+}* heterozygous embryos receiving 10 μg/g RA had 7 cervical vertebrae and the other half had 6 cervical vertebrae (Figure 6E). Finally, RA treatment was required during a specific period on embryonic day 7, as treatment at E8.5 did not rescue the Moz mutant phenotype (data not shown).

RA treatment at E7.25 resulted in stronger expression of *Hoxa1* at E8.5 in *Moz^{Δ/Δ}* mutant embryos than in wild-type controls (Figure S3), which stood in stark contrast to the usual low levels of *Hox* gene expression in *Moz^{Δ/Δ}* mutant embryos without treatment. However, growth retardation by approximately 12 hr at E8.5, which was more severe in wild-type embryos than in *Moz^{Δ/Δ}* mutant embryos, was observed after RA treatment, which complicated the analysis.

Gene expression levels for the rate-limiting enzyme in RA synthesis, *Raldh2*, and the retinoic acid receptors alpha (RARα) and beta were indistinguishable in *Moz^{Δ/Δ}* mutant embryos and controls (data not shown; n = 6 *Moz^{Δ/Δ}* mutant embryos and 6 wild-type embryo per gene). Furthermore, nuclear translocation of the RARα
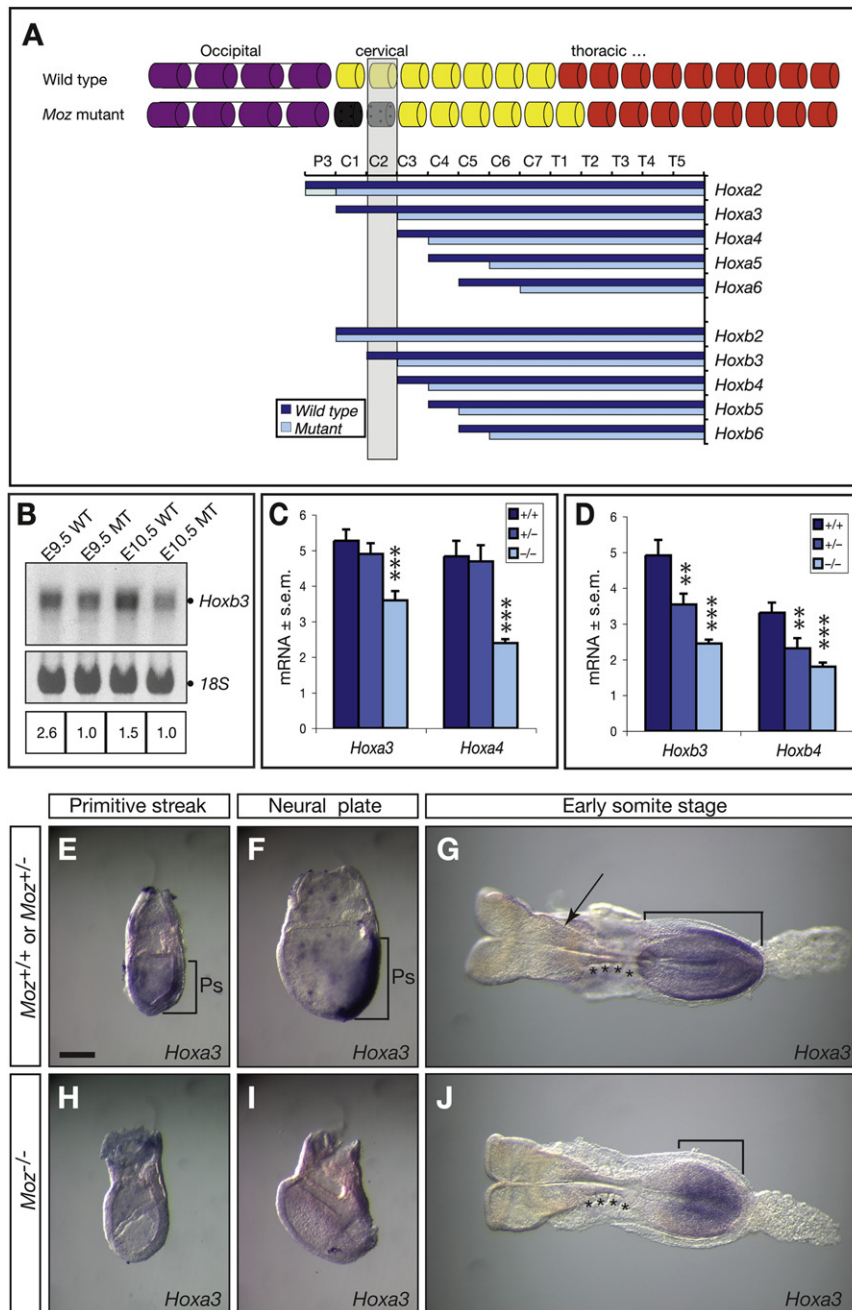
Figure 4. *Hox* Gene Expression in the *Moz^(Δ/Δ)^* Assessed by Whole-Mount In Situ Hybridization and Northern Blot

(A) Diagram of the developing axial skeleton from the 1st occipital to the 9th thoracic segment. Bars show the anterior extent of *Hox* gene expression domains in the paraxial mesoderm at E10.5. Data are shown of a total of 60 wild-type and 60 *Moz^(Δ/Δ)^* embryos, 6 of each genotype for each probe. Note the shift by at least one segment posterior from the 3rd paralogous group onward (*Hoxa3*, *Hoxb3*, and more posteriorly expressed *Hox* genes). Shaded area indicates the first segment, which lost expression of both paralogous genes of *Hox* clusters A and B. The identity of this segment is duly shifted anteriorly (C2→C1).

(B–D) Quantitation of the reduction in *Hox* gene expression in *Moz^(Δ/Δ)^* and controls by northern blot analysis of pooled E9.5 and E10.5 embryos (B) and of individual E11.5 embryos followed by densitometry (C and D) shows an approximately 2-fold reduction in expression of *Hoxa3*, *Hoxa4*, *Hoxb3*, and *Hoxb4* (n = 3 to 5 E11.5 embryos per genotype; p < 0.0001). Data are presented and were analyzed as described in the Experimental Procedures. Error bars show SEM. p values of <0.01 and <0.001 are indicated with two and three asterisks, respectively. At E7.5 *Hoxa3* expression was very low or undetectable in *Moz^(−/−)^* mutants as compared to controls ([E] and [F] versus [H] and [I]) and did not reach the same extent and intensity (G and J). PS, primitive streak; asterisks in (H) and (K) indicate somites; the arrow indicates the hindbrain expression domain of *Hoxa3* detectable in the wild-type. Bars equal 180 μm in (F), (G), (I), and (J) and 200 μm in (H).

the ability of RA to specifically rescue H3K9 acetylation in Moz-deficient embryos.

Ing5, a Moz Protein Complex Component, Occupies *Hox* Loci When Moz Is Present

Human MOZ has been shown to be a part of the ING5 tumor suppressor complex in HeLa cells (Doyon et al., 2006). We observed that mouse Ing5 associated with *Hox* gene loci in the presence, but not in the absence, of Moz (Figure 7L; all *Hox* sites p < 0.0001). RA treatment failed to rescue Ing5 association with *Hox* loci in *Moz* mutants (Figures 7M and 7N; p = 0.0013; Table S3). These data show that Moz is required for Ing5 recruitment to and/or tethering at *Hox* loci.

Mll1 Association with *Hox* Loci Is Reduced in the Absence of Moz

The *TrxG* gene Mll1 is required for *Hox* gene expression, and mutation of *Mll1* leads to an anterior homeotic transformation similar in extent and severity to the anterior homeotic
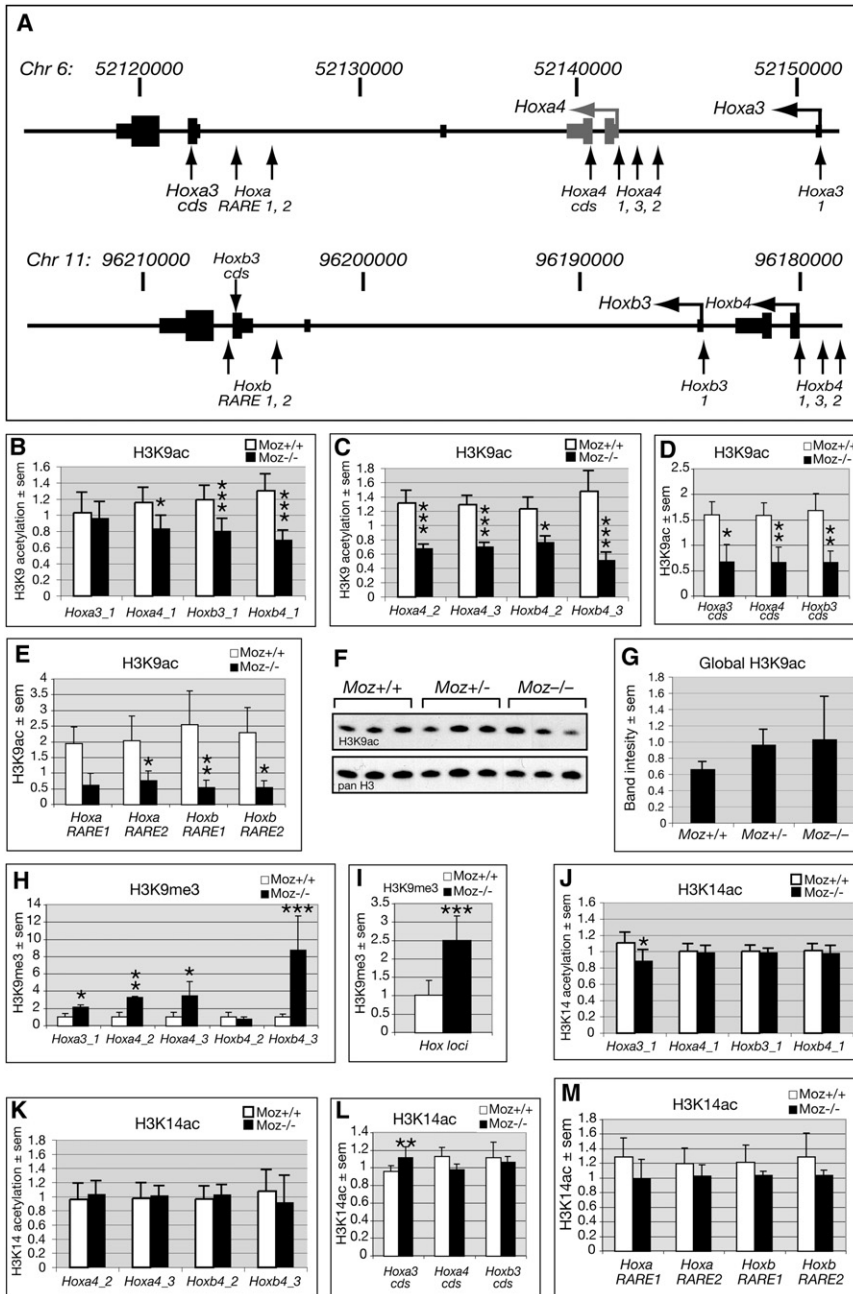
RA treatment (Figures 7I and 7J). RA had no effect on H4K16ac (Figure 7J versus Figure 7I).

Considering levels of H3K9, H3K14, and H4K16 acetylation at all *Hox* sites examined, we can conclude that H3K9ac is reduced in the absence of Moz (Figure 7E; p < 0.0001) and restored to normal by RA (Figure 7E; p < 0.0001), while H3K14ac at all sites is neither affected by Moz nor by RA (Figure 7H; p = 0.2096 and p = 0.4595, respectively) and H4K16ac is increased in the absence of Moz (Figure 7K; p < 0.0001) and not influenced by RA treatment in wild-type or *Moz^(−/−)^* mutants (Figure 7K; p = 0.2861). The data show that Moz specifically acetylates H3K9 and demonstrate

Figure 5. H3K9 Hypoacetylation and Hypermethylation at *Hox* Loci in *Moz*⁻/⁻ Embryos

(A) Genomic region examined for histone modifications and protein binding by ChIP/qPCR. "Hoxa3_1", "Hoxa4_1", "_2," etc denote sequences amplified in (B)–(M) and Figure 7. H3K9ac (B–E), H3K9me3 (H and I) and H3K14ac (J–M) were assessed by ChIP of lysates of *Moz*⁻/⁻ mutant and wild-type E10.5 embryos followed by qPCR of sequences spanning the start of transcription ([B, H, and J], tile_1), 0.7 to 1.5 kb 5′ of the start of transcription ([C, H, and K], tiles_2 and _3), in the protein coding regions ([D and L], cds), and at putative RARE (E and M). Data are derived from a total of 30 embryos, 6 of each genotype for H3K9ac and H3K14ac, 3 of each genotype for H3K9me3. Note the reduction in H3K9ac in *Moz*⁻/⁻ mutant embryos at *Hox* loci overall ([B–E], overall $p < 0.0001$) and the corresponding increase in H3K9me3 ([H and I], overall $p = 0.0004$), but the lack of an effect on H3K14ac ([J–M], overall $p = 0.7155$). (F and G) Global H3K9 acetylation as assessed by immunoblotting (F) and densitometry (G) was not significantly different in the three genotypes (Mr 17 kDA; $p = 0.7109$; $n = 3$ E10.5 embryos per genotype; 1 individual embryo per lane). Data are presented and were analyzed as described in the Experimental Procedures. Error bars represent SEM. For the effect of *Moz* genotype, p values <0.05, <0.01, and <0.001 are indicated with one, two, and three asterisks, respectively. Exact p values are given in Table S2.

DISCUSSION

The MYST histone acetyltransferase MOZ is the target of recurrent translocations causing a particularly aggressive form of acute myeloid leukemia (Borrow et al., 1996; Carapeti et al., 1998; Liang et al., 1998), and Moz is required for the development of hematopoietic stem cells (Katsumoto et al., 2006; Thomas et al., 2006). Here we have shown that Moz is required for normal levels of H3K9 acetylation and gene expression at a large number of *Hox* loci and for identity specification of 19 body segments of the cervical and thoracic axial skeleton and nervous system. Interestingly, the anterior homeotic transformation, *Hox* gene expression, and H3K9 acetylation were completely rescued by treatment of *Moz* mutant embryos with retinoic acid.

Functional Comparison of Mouse Moz and Zebrafish Moz

Our study revealed surprising differences in Moz function in mouse and zebrafish. There is a much more extensive requirement for Moz to activate *Hox* gene expression in mouse embryos (our data presented here) than in zebrafish (Crump et al., 2006; Miller et al., 2004). The lack of an effect on more posterior *hox* genes is commensurate with restricted expression of *moz* in the zebrafish head (Miller et al., 2004). However, the lack of an
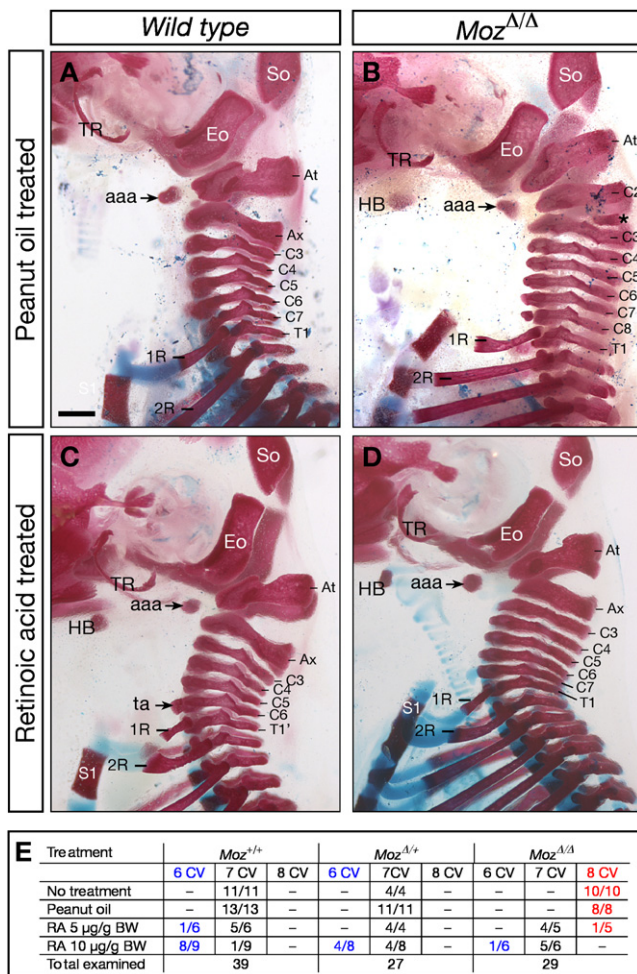
transformation that we observed in the *Moz* mutant mice. In order to address a possible functional link between Moz and Mll1, we assessed occupancy of *Hox* loci by Mll1 in *Moz*⁻/⁻ mutant embryos and controls. Individual *Hox* sites showed a tendency or a mildly significant decrease in association with Mll1 (Figure 7O), which resulted in a significant reduction in association of Mll1 in the absence of Moz when considering all *Hox* sites together (Figure 7P; all *Hox* sites $p = 0.0001$; Table S3).

The observation that the absence of Moz results in reduced association of Mll1 with *Hox* gene loci and reduced *Hox* gene expression suggests that Moz or H3K9 acetylation may recruit Mll1 to *Hox* gene loci.

Figure 6. Retinoic Acid Treatment Rescues the *Moz^{Δ/Δ}* Mutant Body Segment Identity Defect

Skeletal preparations of wild-type (A and C) and *Moz^{Δ/Δ}* (B and D) E18.5 pups. Dams were treated at E7.25 with peanut oil (A and B) or 10 μg/g bodyweight RA in peanut oil (RA, [C and D]). Note the supernumerary cervical vertebra in the peanut-oil-treated *Moz^{Δ/Δ}* ([B] versus [A]), as seen in untreated pups (Figure 1), and the rescue of the cervical vertebrae in the RA-treated *Moz^{Δ/Δ}* ([D] versus [C] and [A]), as well as the reduction of the number of cervical vertebrae to six in the RA-treated wild-type ([C] versus [A]). (E) Enumeration of skeletal preparations. The effects of RA on *Moz^{Δ/Δ}* (rescue), on wild-type (reduction to six cervical vertebrae), and on *Moz^{Δ/+}* heterozygote (reduction to six cervical vertebrae in half the cases) was statistically significant with p < 0.0001, p < 0.0001, and p = 0.009, respectively. Data were analyzed as described in the Experimental Procedures. Labeling as in Figure 1. The scale bar equals 0.6 mm.

effect of zMoz on *hoxa1a* (Miller et al., 2004) cannot be explained by nonoverlapping expression domains and suggests a clear difference in the function of Moz in mice and zebrafish. Effects of the zebrafish *moz* mutation are restricted to the cranial neural crest and the second to fourth pharyngeal arch (Crump et al., 2006; Miller et al., 2004). In contrast, *Moz* mutant mice show identity defects in a total of 19 body segments extending over the cervical and thoracic region. Conversely, unlike in zebrafish, the second pharyngeal arch and the cranial nerves I–XI are unchanged in mouse *Moz* mutants. This may be due to functional

redundancy between Moz and the closely related MYST protein Qkf/Morf/Kat6b, which is particularly strongly expressed in head structures during mouse development (Thomas et al., 2000). Moz and Qkf share all functional domains and have greater than 90% similarity in their PHD, MYST, and serine-rich domains (Thomas et al., 2000). Thus, Qkf may substitute partially for the loss of Moz in head structures.

Moz and Retinoic Acid in *Hox* Gene Regulation

The anterior homeotic transformation in *Moz* mutants observed here is opposite to the posterior homeotic transformation caused by teratogenic treatment with RA (Kessel and Gruss, 1991). RA is a potent, global activator of *Hox* gene expression. Oversupply of RA or vitamin A leads to birth defects in humans (Geelen, 1979). RA is produced by the developing embryo (Hogan et al., 1992) and degraded by Cyp26 to generate specific RA levels along the rostro-caudal body axis (Sakai et al., 2001). RA acts through retinoic acid receptors (RAR), which are expressed in partially overlapping patterns along the rostro-caudal axis of the embryo (Dolle et al., 1990; Ruberte et al., 1991). RAR translocate to the nucleus, where they binds to retinoic acid response elements (RARE). A number of RARE within the *Hox* clusters have been functionally verified in vivo by showing that *Hox* gene RARE reporter transgenes recapitulate the specific anterior expression boundary of the original *Hox* gene in vivo (Dupe et al., 1997; Gould et al., 1998; Huang et al., 2002; Marshall et al., 1994; Packer et al., 1998; Zhang et al., 2000).

Interestingly, we found that the elements of the RA signaling pathway functioned in the absence of Moz. However, the MOZ-TIF2 fusion protein, which causes leukemia, downregulates the transcription of the *RARβ* gene (Collins et al., 2006). The absence of an effect of Moz deficiency on *RARβ* gene expression suggests that the oncogenic MOZ-TIF2 fusion protein has acquired an ectopic function. In contrast, *RAR* genes are expressed normally and RAR translocates into the nucleus normally in *Moz* mutant embryos. Most importantly, the *Moz* mutant segment identity defect is rescued by RA treatment. This shows that at least exogenous RA can act through its receptors and activate *Hox* gene expression in the absence of Moz.

Moz, Polycomb Group, and Trithorax Group Proteins in *Hox* Gene Regulation

PcG proteins act in multiprotein complexes, the polycomb repressor complexes. They add the repressive histone modification H3K27me3 and are required to maintain repression of *Hox* genes. Mutations of proteins of the polycomb complex cause deregulation of *Hox* gene expression and posterior homeotic transformations, as seen for example in *Bmi1*, *Mel18*, and *Eed* mutants (Akasaka et al., 1996; Schumacher et al., 1996; van der Lugt et al., 1994). The polycomb group protein Eed associates with histone deacetylase activity (van der Vlag and Otte, 1999), the enzymatic activity directly opposing the action of histone acetyltransferases. Mutations of polycomb complex proteins and mutation of *Moz* cause opposite effects: posterior versus anterior homeotic transformation; deregulation of *Hox* gene activity versus loss of *Hox* gene activity.

Directly opposing the function of polycomb repressor complexes, proteins of the trithorax group (TrxG) add the histone
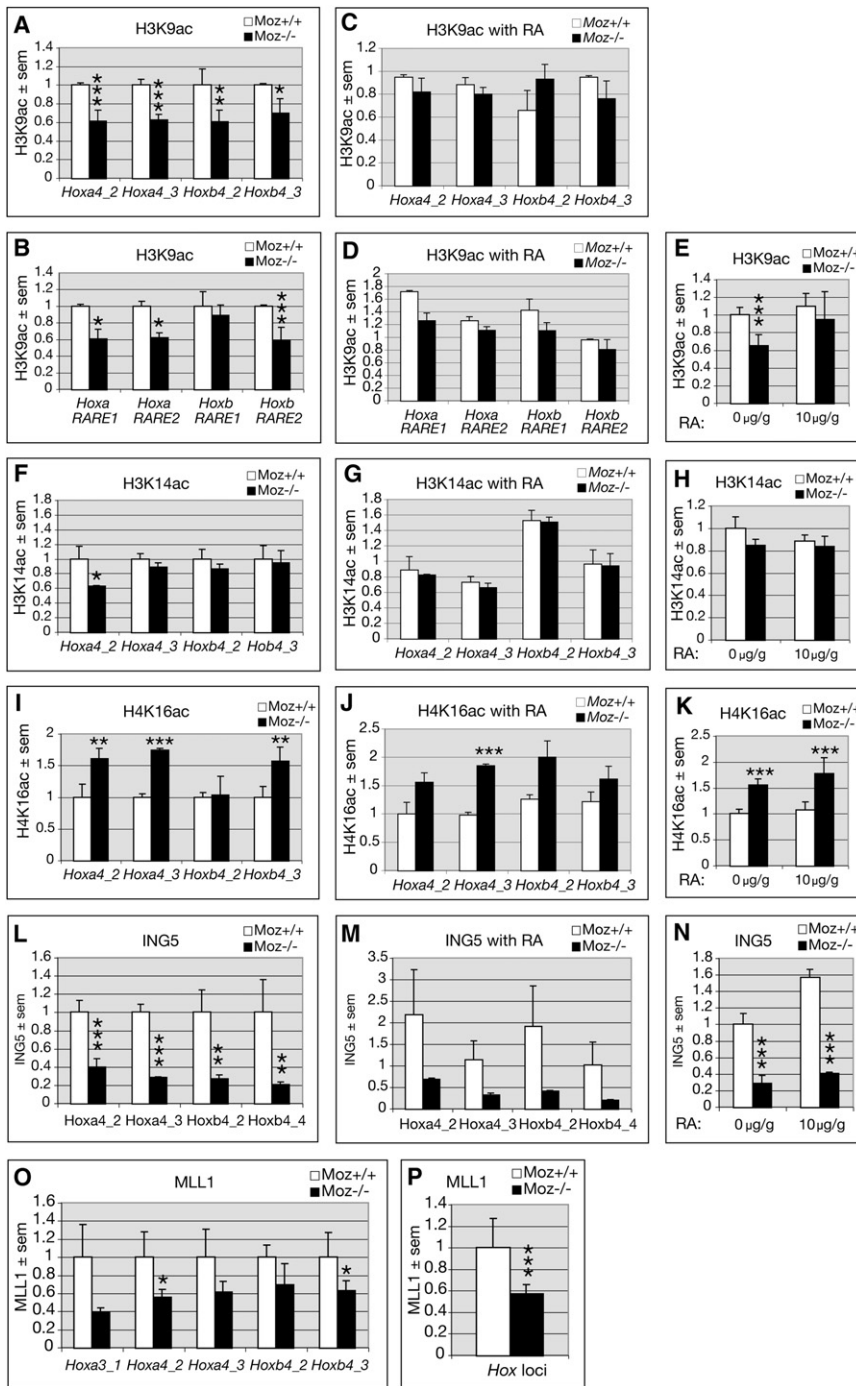
Figure 7. Retinoic Acid Treatment of *Moz*$^{-/-}$ Mutants at E9.5 Restores H3K9 Acetylation at E10.5, and Recruitment of Ing5 and Mll1 Are Dependent on Moz

E10.5 embryos were used for ChIP experiments (A–P) as in Figures 5O and 5P) or after treatment of the pregnant females with vehicle (peanut oil) or RA at E9.5. H3K9 (A–E), H3K14 (F–H), and H4K16 (I–K) acetylation and Ing5 (L–N) and Mll1 association (O and P) were assessed at a subset of the genomic *Hox* sites examined in Figure 5. Effects summarized over all genomic sites are displayed (E, H, K, N, and P). Note the reduction in H3K9ac in *Moz*$^{-/-}$ mutants without RA as compared to controls (A, B, and E) and the similar levels of H3K9ac after RA treatment (C, D, and E), whereas H4K16ac is increased in *Moz*$^{-/-}$ mutants and not affected by RA treatment (I–K). In contrast to H3K9ac and H4K16ac, H3K14ac is generally not different between *Moz*$^{-/-}$ mutants and controls irrespective of RA (F–H). Note the very low levels of Ing5 association with *Hox* loci in *Moz*$^{-/-}$ mutants as compared to controls (L and N). RA treatment did not rescue the levels of Ing5 at *Hox* loci in *Moz*$^{-/-}$ mutants (M and N). Note the reduction in the TrxG protein Mll1 at *Hox* loci in *Moz*$^{-/-}$ mutants as compared to controls (O and P). For the effect of *Moz* genotype, p values are indicated as in Figure 5, and exact p values are in Table S3. Error bars represent SEM.

acetylated at K9 (and K14), whereas H3K9 methylation reduces its association with H3 in vitro (Katsani et al., 2001). Moreover, H3 peptide acetylated at H3K9 stimulates the H3K4-methyltransferase activity of the MLL1 SET domain in vitro (Milne et al., 2002). Together, these results suggest a complex interplay between H3K9 acetylation and H3K4 methylation.

Moz-Specific Histone Acetylation Marks

MOZ has been reported to acetylate histones H2A, H2B, H3, and H4 in the form of free histones in vitro (Champagne et al., 2001; Holbert et al., 2007; Laue et al., 2008). MOZ can acetylate lysines 5, 8, 12, and 16 of histone H4 and lysine 14 of histone H3 in vitro (Kitabayashi et al., 2001). Specific histone residues put forward as preferential targets of MOZ include H4K16 when comparing normal lymphocytes to leukemia cells (Fraga et al., 2005) and H3K14 in HeLa cell extracts (Doyon et al., 2006). H3K9 was previously ruled out as a MOZ acetylation target (Doyon et al., 2006). However, our comparison of H3K9, H3K14, and H4K16 acetylation in the Moz-replete and Moz-deficient embryos shows that Moz is required specifically for H3K9 acetylation at *Hox* loci in vivo. H3K9 acetylation was reduced by approximately one half in *Moz* mutants, suggesting the presence of another H3K9

methylation mark typical of transcriptionally active loci, H3K4me3. Like mutations of the *Moz* gene, mutations of *TrxG* genes lead to hematopoietic malignancies. The anterior homeotic transformation that we observed in the Moz mutants is rivaled in completeness and extent only by mutation of the *Mll1* gene (Yu et al., 1995). We show here that not only is Moz required for normal *Hox* gene expression and body segment identity specification, like TrxG proteins, but Moz is also required for the association of Mll1 with *Hox* gene loci in vivo. Indeed, the SET domain of MLL1 binds with preference to H3 when

acetyltransferase, possibly the closely related Qkf protein with which Moz shares all functional domains.

Remarkably, RA treatment restored H3K9 acetylation levels and *Hox* gene expression levels in the *Moz* mutant embryos. Although the identity of the histone acetyltransferase activity that acetylates H3K9 specifically at *Hox* loci in conjunction with RA signaling in the absence of Moz is currently unclear, the nuclear receptor coactivator 3 (NCOA3/ACTR/KAT13B) associates with retinoic acid receptors, is a histone acetyltransferase, and also recruits additional histone acetyltransferases upon retinoic acid and hormone stimulation in a number of human and rat cell lines (Chen et al., 1997; Torchia et al., 1997). In contrast to H3K9, there were few or no effects of either Moz or RA on H3K14 acetylation. In the case of an indirect effect of Moz (or RA) on transcriptional activation of *Hox* genes, one would have expected effects on several activation marks. The specificity of the action of Moz (and RA) on H3K9, but not on H3K14, and the direct binding of Ing5, a member of the Moz protein complex, to *Hox* loci suggest that Moz directly acetylates H3K9 at *Hox* loci. Whether Moz is also responsible for acetylation of histone residues other than H3K9 in vivo at other stages of development or other loci remains to be examined. Furthermore, it will be interesting to examine occupation of *Hox* loci by Moz protein, once ChIP-grade antibodies specific to Moz become available.

The *Hoxd4* locus acquires H3 acetylation marks of transcriptionally active loci *before* onset of transcription during mouse development (Rastegar et al., 2004). Similarly, H3K9ac and H3K4me2 were found in the *Hoxb9* locus *before* transcriptional activation in RA-induced embryonic stem cells (Chambeyron and Bickmore, 2004). These findings suggest that major regulators of *Hox* gene expression such as TrxG proteins, previously perceived as having a maintenance but not an initiation function, may initiate chromatin changes at *Hox* loci in mouse development even before *Hox* genes are activated. Our data show that Moz is required not only for the maintenance of normal *Hox* gene expression patterns and levels, but also for very early *Hox* gene expression, and they support the idea of a requirement for Moz and H3K9 acetylation for the onset of gene transcription.

The complex time/space patterns of gene expression necessary for normal development are likely to require multiple epigenetic signals. H3K9 is a substrate for both acetylation and methylation, and indeed, in the absence of Moz the transcription repressive mark, H3K9 trimethylation, is correspondingly elevated. Acetylation of H3K9 correlates with induction of gene expression (Agalioti et al., 2002). In contrast, methylation of H3K9 can lead to the recruitment of silencing proteins (Bannister et al., 2001; Lachner et al., 2001) and is directly linked to DNA methylation in a number of human cell lines (Esteve et al., 2006). Since the presence of acetylation at H3K9 precludes methylation, the action of Moz in the *Hox* loci may generate and stabilize a pattern of chromatin modifications required for *Hox* gene expression.

In HeLa cells, the MYST histone acetyltransferase MOF and the TrxG protein MLL1 are physically associated and act on the core histones in a coordinated manner, with MLL1 methylating H3K4 and MOF acetylating H4K16 (Dou et al., 2005). Our data presented here show that Moz is required for the association of Mll1 with *Hox* gene chromatin. In contrast, H4K16 acetylation was not dependent on Moz. We have shown previously that Mof specifically acetylates H4K16 and opposes global chromatin condensation during mammalian embryonic development (Thomas et al., 2008). The fact that H4K16 was hyperacetylated in the absence of Moz suggests that another histone acetyltransferase, possibly Mof, hyperacetylates H4K16 in the absence of Moz. Based on our finding presented here, we propose that Moz and Mll1 act in concert to induce and maintain *Hox* gene expression and that Moz is the H3K9-acetyltransferase opposing the histone deacetylase activity associated with polycomb repressor complexes.

In conclusion we have shown that (1) Moz is required for normal levels and spatially correct *Hox* gene expression, (2) Moz is required for correct body segment identity specification of 19 body segments, and (3) RA rescues the *Moz* mutant body segment identity defect. Furthermore we have demonstrated that (4) Moz is specifically required for the H3K9 acetylation mark of transcriptionally active *Hox* gene loci, (5) in the absence of Moz the transcriptionally repressive H3K9 trimethylation mark is propagated, and (6) Moz is required for the presence of Mll1 and Ing5 at *Hox* loci.

EXPERIMENTAL PROCEDURES

$Moz^{\Delta/+}$ (Thomas et al., 2006) and $Moz^{+/-}$ (Figure S4) heterozygous mice on C57BL/6, 129/Sv inbred and FVB/BALB/c hybrid backgrounds were used for this study. The anterior homeotic transformation of the axial skeleton was present in *Moz* mutant pups on all genetic backgrounds. Mice were mated and examined for vaginal plugs 2 hr after mating (to exclude afternoon matings) and then daily in the morning. Noon of the morning observation of a vaginal plug was termed E0.5. Embryos and pups were collected at the developmental stages indicated in text and figure legends, and extraembryonic membranes were used for genotyping by three-way PCR as we described previously (Thomas et al., 2006) and as indicated in Figure S4.

Skeletal preps were conducted as described previously (Thomas et al., 2000). Whole-mount in situ hybridization was carried out as described (Thomas et al., 2007). Sense and antisense probes for *Moz*, *Hox* genes from *Hoxa1* to *a6* and *Hoxb2* to *b6* and *Hoxb8* were used. cRNA probes are listed in Table S4. Whole-mount immunohistochemistry was performed as described previously (Loughran et al., 2008). Total RNA isolation, northern blot analysis, and densitometry were conducted as described previously (Voss et al., 2000).

Doses for RA treatment were established in pilot experiments. RA in sterile peanut oil was mixed with powdered mouse feed and replaced the normal feed. RA feed was consumed within 6 hr after treatment at 8:00 am (2 hr after the dark/light switch). We tested doses of 5, 10, 20, and 40 μg RA per gram of bodyweight versus peanut oil treatment without RA. We observed reliable development of RA-treated pups to E18.5 only at the two lowest doses, consistent with findings by Kessel and Gruss (1991).

Chromatin immunoprecipitation (ChIP) was carried out according to the Upstate ChIP protocol (cat# 17-295) with modifications as described in the Supplemental Experimental Procedures followed by genomic qPCR using primers listed in Table S5.

Antibodies used for ChIP and immunoblotting were directed against MLL1 (Bethyl A300-086A), ING5 (Abnova H00084289-B01), H3K9ac (Millipore, Upstate 07-352), H3K14ac (Millipore, Upstate 07-353), H4K16ac (Millipore P62805), and H3K9me3 (Abcam ab8898). These anti-histone antibodies detect the modified histone preferentially over other forms of the same histone. Anti-pan H3 (Millipore, Upstate 05-858) was used as a loading control in immunoblotting, and anti-IgG was used as a control in ChIP. Antibodies used for whole-mount immunohistochemistry and immunofluorescence were directed against neurofilament (clone 2H3 supplied by T.M. Jessel and J. Dodd to the Developmental Studies Hybridoma Bank [DSHB], University of Iowa), Hoxb4 (clone I12 supplied by A Gould and R Krumlauf to DSHB) and RARα (Abnova H5914-M03 1:400).

Total protein isolation, SDS polyacrylamide gel electrophoresis, and western blot analysis were carried out as described previously (Voss et al., 2003). Immunofluorescence was conducted as described previously (Voss et al., 2003).

Putative retinoic acid receptor response elements (RARE) near the *Hoxa3* and *Hoxb3* locus were selected using a Hidden Markov Model-based algorithm published and implemented in a web interface by Sandelin and Wasserman (2005) (http://www.cisreg.ca/cgi-bin/NHR-scan/nhr_scan.cgi). We then examined the sequence conservation of the predicted RARE between human, mouse, rat, and dog. As the first *Hox* gene in the *Hoxa* and the *Hoxb* cluster with changes in the anterior expression boundary in *Moz* mutants was in the third paralogous group, we selected two putative RARE each in the vicinity of the *Hoxa3* and the *Hoxb3* loci, respectively, based on sequence conservation for ChIP analysis (Table S1). *HoxaRARE-1, -2,* and *HoxbRARE-2* are 100% conserved between human, dog, mouse, and rat. Ten and twelve of thirteen bases of *HoxbRARE-1* are conserved between humans versus the rodent species and dog, respectively. *HoxbRARE-1* is a perfect consensus RARE as described (Mangelsdorf et al., 1995; Packer et al., 1998), while the other three differ by one nucleotide each (Table S1).

Data were analyzed using Intercooled Stata 10 software. Densitometry data are presented as means ± SEM of densitometry readings and were analyzed by two or three-factorial analysis of variance (ANOVA) with the number of intact *Moz* alleles and animal as two independent factors with or without *Hox* gene locus as a third independent factor, followed by Scheffe's post-hoc test. ChIP/qPCR data are presented as standardized means ± SEM of DNA concentration normalized for the housekeeping genes *beta-2-microglobulin* (for active marks) or *albumin* and *hemoglobin b1* (for repressive marks) and were analyzed by one-, two- or three-factorial ANOVA with repeats with number of intact Moz alleles as the first independent factor, with or without *Hox* gene locus as a second independent factor, and with or without retinoic acid as a third independent factor, followed by Scheffe's post-hoc test. Frequencies of numbers of cervical vertebrae in RA-treated versus peanut-oil-treated or untreated *Moz* mutants and controls were compared by χ^2 test. Data in Figure 7 were normalized to untreated wild-type to allow cross-comparison not just between genotypes, but also between retinoic acid treatment groups. The large number of exact p values corresponding to individual genomic sites in Figures 5 and 7 are given in Tables S2 and S3 to increase readability of the text.

SUPPLEMENTAL DATA

Supplemental Data include four figures, five tables, and Supplemental Experimental Procedures and can be found with this article online at http://www.cell.com/developmental-cell/supplemental/S1534-5807(09)00428-6/.

REFERENCES

Agalioti, T., Chen, G., and Thanos, D. (2002). Deciphering the transcriptional histone acetylation code for a human gene. Cell *111*, 381–392.

Akasaka, T., Kanno, M., Balling, R., Mieza, M.A., Taniguchi, M., and Koseki, H. (1996). A role for mel-18, a Polycomb group-related vertebrate gene, during theanteroposterior specification of the axial skeleton. Development *122*, 1513–1522.

Bannister, A.J., Zegerman, P., Partridge, J.F., Miska, E.A., Thomas, J.O., Allshire, R.C., and Kouzarides, T. (2001). Selective recognition of methylated lysine 9 on histone H3 by the HP1 chromo domain. Nature *410*, 120–124.

Borrow, J., Stanton, V.J., Andresen, J., Becher, R., Behm, F., Chaganti, R., Civin, C., Disteche, C., Dube, I., Frischauf, A., et al. (1996). The translocation t(8;16)(p11;p13) of acute myeloid leukaemia fuses a putative acetyltransferase to the CREB-binding protein. Nat. Genet. *14*, 33–41.

Carapeti, M., Aguiar, R., Goldman, J., and Cross, N. (1998). A novel fusion between MOZ and the nuclear receptor coactivator TIF2 in acute myeloid leukemia. Blood *91*, 3127–3133.

Chaffanet, M., Gressin, L., Preudhomme, C., Soenen-Cornu, V., Birnbaum, D., and Pebusque, M.J. (2000). MOZ is fused to p300 in an acute monocytic leukemia with t(8;22). Genes Chromosomes Cancer *28*, 138–144.

Chambeyron, S., and Bickmore, W.A. (2004). Chromatin decondensation and nuclear reorganization of the HoxB locus upon induction of transcription. Genes Dev. *18*, 1119–1130.

Champagne, N., Pelletier, N., and Yang, X.J. (2001). The monocytic leukemia zinc finger protein MOZ is a histone acetyltransferase. Oncogene *20*, 404–409.

Chen, H., Lin, R.J., Schiltz, R.L., Chakravarti, D., Nash, A., Nagy, L., Privalsky, M.L., Nakatani, Y., and Evans, R.M. (1997). Nuclear receptor coactivator ACTR is a novel histone acetyltransferase and forms a multimeric activation complex with P/CAF and CBP/p300. Cell *90*, 569–580.

Collins, H.M., Kindle, K.B., Matsuda, S., Ryan, C., Troke, P.J., Kalkhoven, E., and Heery, D.M. (2006). MOZ-TIF2 alters cofactor recruitment and histone modification at the RARbeta2 promoter: differential effects of MOZ fusion proteins on CBP- and MOZ-dependent activators. J. Biol. Chem. *281*, 17124–17133.

Condie, B.G., and Capecchi, M.R. (1994). Mice with targeted disruptions in the paralogous genes hoxa-3 and hoxd-3 reveal synergistic interactions. Nature *370*, 304–307.

Crump, J.G., Swartz, M.E., Eberhart, J.K., and Kimmel, C.B. (2006). Moz-dependent Hox expression controls segment-specific fate maps of skeletal precursors in the face. Development *133*, 2661–2669.

Deschamps, J., and van Nes, J. (2005). Developmental regulation of the Hox genes during axial morphogenesis in the mouse. Development *132*, 2931–2942.

Dolle, P., Ruberte, E., Leroy, P., Morriss-Kay, G., and Chambon, P. (1990). Retinoic acid receptors and cellular retinoid binding proteins. I. A systematic study of their differential pattern of transcription during mouse organogenesis. Development *110*, 1133–1151.

Dou, Y., Milne, T.A., Tackett, A.J., Smith, E.R., Fukuda, A., Wysocka, J., Allis, C.D., Chait, B.T., Hess, J.L., and Roeder, R.G. (2005). Physical association and coordinate function of the H3 K4 methyltransferase MLL1 and the H4 K16 acetyltransferase MOF. Cell *121*, 873–885.

Doyon, Y., Cayrou, C., Ullah, M., Landry, A.J., Cote, V., Selleck, W., Lane, W.S., Tan, S., Yang, X.J., and Cote, J. (2006). ING tumor suppressor proteins are critical regulators of chromatin acetylation required for genome expression and perpetuation. Mol. Cell *21*, 51–64.

Dupe, V., Davenne, M., Brocard, J., Dolle, P., Mark, M., Dierich, A., Chambon, P., and Rijli, F.M. (1997). In vivo functional analysis of the Hoxa-1 3′ retinoic acid response element (3′RARE). Development *124*, 399–410.

Esteve, P.O., Chin, H.G., Smallwood, A., Feehery, G.R., Gangisetty, O., Karpf, A.R., Carey, M.F., and Pradhan, S. (2006). Direct interaction between DNMT1 and G9a coordinates DNA and histone methylation during replication. Genes Dev. *20*, 3089–3103.

Esteyries, S., Perot, C., Adelaide, J., Imbert, M., Lagarde, A., Pautas, C., Olschwang, S., Birnbaum, D., Chaffanet, M., and Mozziconacci, M.J. (2008). NCOA3, a new fusion partner for MOZ/MYST3 in M5 acute myeloid leukemia. Leukemia *22*, 663–665.

Fraga, M.F., Ballestar, E., Villar-Garea, A., Boix-Chornet, M., Espada, J., Schotta, G., Bonaldi, T., Haydon, C., Ropero, S., Petrie, K., et al. (2005). Loss of acetylation at Lys16 and trimethylation at Lys20 of histone H4 is a common hallmark of human cancer. Nat. Genet. *37*, 391–400.

Fromental-Ramain, C., Warot, X., Lakkaraju, S., Favier, B., Haack, H., Birling, C., Dierich, A., Dollé, P., and Chambon, P. (1996). Specific and redundant functions of the paralogous Hoxa-9 and Hoxd-9 genes in forelimb and axial skeleton patterning. Development *122*, 461–472.

Geelen, J.A. (1979). Hypervitaminosis A induced teratogenesis. CRC Crit. Rev. Toxicol. *6*, 351–375.

Gould, A., Itasaki, N., and Krumlauf, R. (1998). Initiation of rhombomeric Hoxb4 expression requires induction by somites and a retinoid pathway. Neuron *21*, 39–51.

Hogan, B.L., Thaller, C., and Eichele, G. (1992). Evidence that Hensen's node is a site of retinoic acid synthesis. Nature *359*, 237–241.

Holbert, M.A., Sikorski, T., Carten, J., Snowflack, D., Hodawadekar, S., and Marmorstein, R. (2007). The human monocytic leukemia zinc finger histone acetyltransferase domain contains DNA-binding activity implicated in chromatin targeting. J. Biol. Chem. *282*, 36603–36613.

Horan, G.S., Ramirez-Solis, R., Featherstone, M.S., Wolgemuth, D.J., Bradley, A., and Behringer, R.R. (1995). Compound mutants for the paralogous hoxa-4, hoxb-4, and hoxd-4 genes show more complete homeotic transformations and a dose-dependent increase in the number of vertebrae transformed. Genes Dev. *9*, 1667–1677.

Huang, D., Chen, S.W., and Gudas, L.J. (2002). Analysis of two distinct retinoic acid response elements in the homeobox gene Hoxb1 in transgenic mice. Dev. Dyn. *223*, 353–370.

Jenuwein, T., and Allis, C.D. (2001). Translating the histone code. Science *293*, 1074–1080.

Katsani, K.R., Arredondo, J.J., Kal, A.J., and Verrijzer, C.P. (2001). A homeotic mutation in the trithorax SET domain impedes histone binding. Genes Dev. *15*, 2197–2202.

Katsumoto, T., Aikawa, Y., Iwama, A., Ueda, S., Ichikawa, H., Ochiya, T., and Kitabayashi, I. (2006). MOZ is essential for maintenance of hematopoietic stem cells. Genes Dev. *20*, 1321–1330.

Kessel, M., and Gruss, P. (1991). Homeotic transformations of murine vertebrae and concomitant alteration of Hox codes induced by retinoic acid. Cell *67*, 89–104.

Kitabayashi, I., Aikawa, Y., Nguyen, L.A., Yokoyama, A., and Ohki, M. (2001). Activation of AML1-mediated transcription by MOZ and inhibition by the MOZ-CBP fusion protein. EMBO J. *20*, 7184–7196.

Lachner, M., and Jenuwein, T. (2002). The many faces of histone lysine methylation. Curr. Opin. Cell Biol. *14*, 286–298.

Lachner, M., O'Carroll, D., Rea, S., Mechtler, K., and Jenuwein, T. (2001). Methylation of histone H3 lysine 9 creates a binding site for HP1 proteins. Nature *410*, 116–120.

Laue, K., Daujat, S., Crump, J.G., Plaster, N., Roehl, H.H., Kimmel, C.B., Schneider, R., and Hammerschmidt, M. (2008). The multidomain protein Brpf1 binds histones and is required for Hox gene expression and segmental identity. Development *135*, 1935–1946.

Liang, J., Prouty, L., Williams, B.J., Dayton, M.A., and Blanchard, K.L. (1998). Acute mixed lineage leukemia with an inv(8)(p11q13) resulting in fusion of the genes for MOZ and TIF2. Blood *92*, 2118–2122.

Loughran, S.J., Kruse, E.A., Hacking, D.F., de Graaf, C.A., Hyland, C.D., Willson, T.A., Henley, K.J., Ellis, S., Voss, A.K., Metcalf, D., et al. (2008). The transcription factor Erg is essential for definitive hematopoiesis and the function of adult hematopoietic stem cells. Nat. Immunol. *9*, 810–819.

Mangelsdorf, D.J., Thummel, C., Beato, M., Herrlich, P., Schutz, G., Umesono, K., Blumberg, B., Kastner, P., Mark, M., Chambon, P., et al. (1995). The nuclear receptor superfamily: the second decade. Cell *83*, 835–839.

Marshall, H., Studer, M., Popperl, H., Aparicio, S., Kuroiwa, A., Brenner, S., and Krumlauf, R. (1994). A conserved retinoic acid response element required for early expression of the homeobox gene Hoxb-1. Nature *370*, 567–571.

Miller, C.T., Maves, L., and Kimmel, C.B. (2004). Moz regulates Hox expression and pharyngeal segmental identity in zebrafish. Development *131*, 2443–2461.

Milne, T.A., Briggs, S.D., Brock, H.W., Martin, M.E., Gibbs, D., Allis, C.D., and Hess, J.L. (2002). MLL targets SET domain methyltransferase activity to Hox gene promoters. Mol. Cell *10*, 1107–1117.

Nakamura, T., Mori, T., Tada, S., Krajewski, W., Rozovskaia, T., Wassell, R., Dubois, G., Mazo, A., Croce, C.M., and Canaani, E. (2002). ALL-1 is a histone methyltransferase that assembles a supercomplex of proteins involved in transcriptional regulation. Mol. Cell *10*, 1119–1128.

Packer, A.I., Crotty, D.A., Elwell, V.A., and Wolgemuth, D.J. (1998). Expression of the murine Hoxa4 gene requires both autoregulation and a conserved retinoic acid response element. Development *125*, 1991–1998.

Pollard, S.L., and Holland, P.W. (2000). Evidence for 14 homeobox gene clusters in human genome ancestry. Curr. Biol. *10*, 1059–1062.

Rastegar, M., Kobrossy, L., Kovacs, E.N., Rambaldi, I., and Featherstone, M. (2004). Sequential histone modifications at Hoxd4 regulatory regions distinguish anterior from posterior embryonic compartments. Mol. Cell. Biol. *24*, 8090–8103.

Ringrose, L., and Paro, R. (2004). Epigenetic regulation of cellular memory by the Polycomb and Trithorax group proteins. Annu. Rev. Genet. *38*, 413–443.

Ringrose, L., and Paro, R. (2007). Polycomb/Trithorax response elements and epigenetic memory of cell identity. Development *134*, 223–232.

Ringrose, L., Ehret, H., and Paro, R. (2004). Distinct contributions of histone H3 lysine 9 and 27 methylation to locus-specific stability of polycomb complexes. Mol. Cell *16*, 641–653.

Ruberte, E., Dolle, P., Chambon, P., and Morriss-Kay, G. (1991). Retinoic acid receptors and cellular retinoid binding proteins. II. Their differential pattern of transcription during early morphogenesis in mouse embryos. Development *111*, 45–60.

Sakai, Y., Meno, C., Fujii, H., Nishino, J., Shiratori, H., Saijoh, Y., Rossant, J., and Hamada, H. (2001). The retinoic acid-inactivating enzyme CYP26 is essential for establishing an uneven distribution of retinoic acid along the anterio-posterior axis within the mouse embryo. Genes Dev. *15*, 213–225.

Sandelin, A., and Wasserman, W.W. (2005). Prediction of nuclear hormone receptor response elements. Mol. Endocrinol. *19*, 595–606.

Schneuwly, S., Klemenz, R., and Gehring, W.J. (1987). Redesigning the body plan of Drosophila by ectopic expression of the homoeotic gene Antennapedia. Nature *325*, 816–818.

Schumacher, A., Faust, C., and Magnuson, T. (1996). Positional cloning of a global regulator of anterior-posterior patterning in mice. Nature *383*, 250–253.

Struhl, G. (1981). A homoeotic mutation transforming leg to antenna in Drosophila. Nature *292*, 635–638.

Thomas, T., and Voss, A.K. (2007). The diverse biological roles of MYST histone acetyltransferase family proteins. Cell Cycle *6*, 696–704.

Thomas, T., Voss, A.K., Chowdhury, K., and Gruss, P. (2000). Querkopf, a MYST family histone acetyltransferase, is required for normal cerebral cortex development. Development *127*, 2537–2548.

Thomas, T., Corcoran, L.M., Gugasyan, R., Dixon, M.P., Brodnicki, T., Nutt, S.L., Metcalf, D., and Voss, A.K. (2006). Monocytic leukemia zinc finger protein is essential for the development of long-term reconstituting hematopoietic stem cells. Genes Dev. *20*, 1175–1186.

Thomas, T., Loveland, K.L., and Voss, A.K. (2007). The genes coding for the MYST family histone acetyltransferases, Tip60 and Mof, are expressed at high levels during sperm development. Gene Expr. Patterns *7*, 657–665.

Thomas, T., Dixon, M.P., Kueh, A.J., and Voss, A.K. (2008). Mof (MYST1 or KAT8) is essential for progression of embryonic development past the blastocyst stage and required for normal chromatin architecture. Mol. Cell. Biol. *28*, 5093–5105.

Torchia, J., Rose, D.W., Inostroza, J., Kamei, Y., Westin, S., Glass, C.K., and Rosenfeld, M.G. (1997). The transcriptional co-activator p/CIP binds CBP and mediates nuclear-receptor function. Nature *387*, 677–684.

van der Lugt, N.M., Domen, J., Linders, K., van Roon, M., Robanus-Maandag, E., te Riele, H., van der Valk, M., Deschamps, J., Sofroniew, M., van Lohuizen, M., et al. (1994). Posterior transformation, neurological abnormalities, and

severe hematopoietic defects in mice with a targeted deletion of the bmi-1 proto-oncogene. Genes Dev. *8*, 757–769.

van der Vlag, J., and Otte, A.P. (1999). Transcriptional repression mediated by the human polycomb-group protein EED involves histone deacetylation. Nat. Genet. *23*, 474–478.

Voss, A.K., and Thomas, T. (2009). MYST family histone acetyltransferases take center stage in stem cells and development. Bioessays *31*, 1050–1061.

Voss, A.K., Thomas, T., and Gruss, P. (2000). Mice lacking HSP90beta fail to develop a placental labyrinth. Development *127*, 1–11.

Voss, A.K., Gruss, P., and Thomas, T. (2003). The guanine nucleotide exchange factor C3G is necessary for the formation of focal adhesions and vascular maturation. Development *130*, 355–367.

Yu, B.D., Hess, J.L., Horning, S.E., Brown, G.A., and Korsmeyer, S.J. (1995). Altered Hox expression and segmental identity in Mll-mutant mice. Nature *378*, 505–508.

Zhang, F., Nagy Kovacs, E., and Featherstone, M.S. (2000). Murine hoxd4 expression in the CNS requires multiple elements including a retinoic acid response element. Mech. Dev. *96*, 79–89.